Figure S1. (A) Cell cycle distribution following treatment with various concentrations of neferine for 24 h, as determined via flow cytometry. (B and C) Effects of different neferine concentrations on the healing and migration of head and neck squamous cell carcinoma cells. *P<0.05 and **P<0.01.

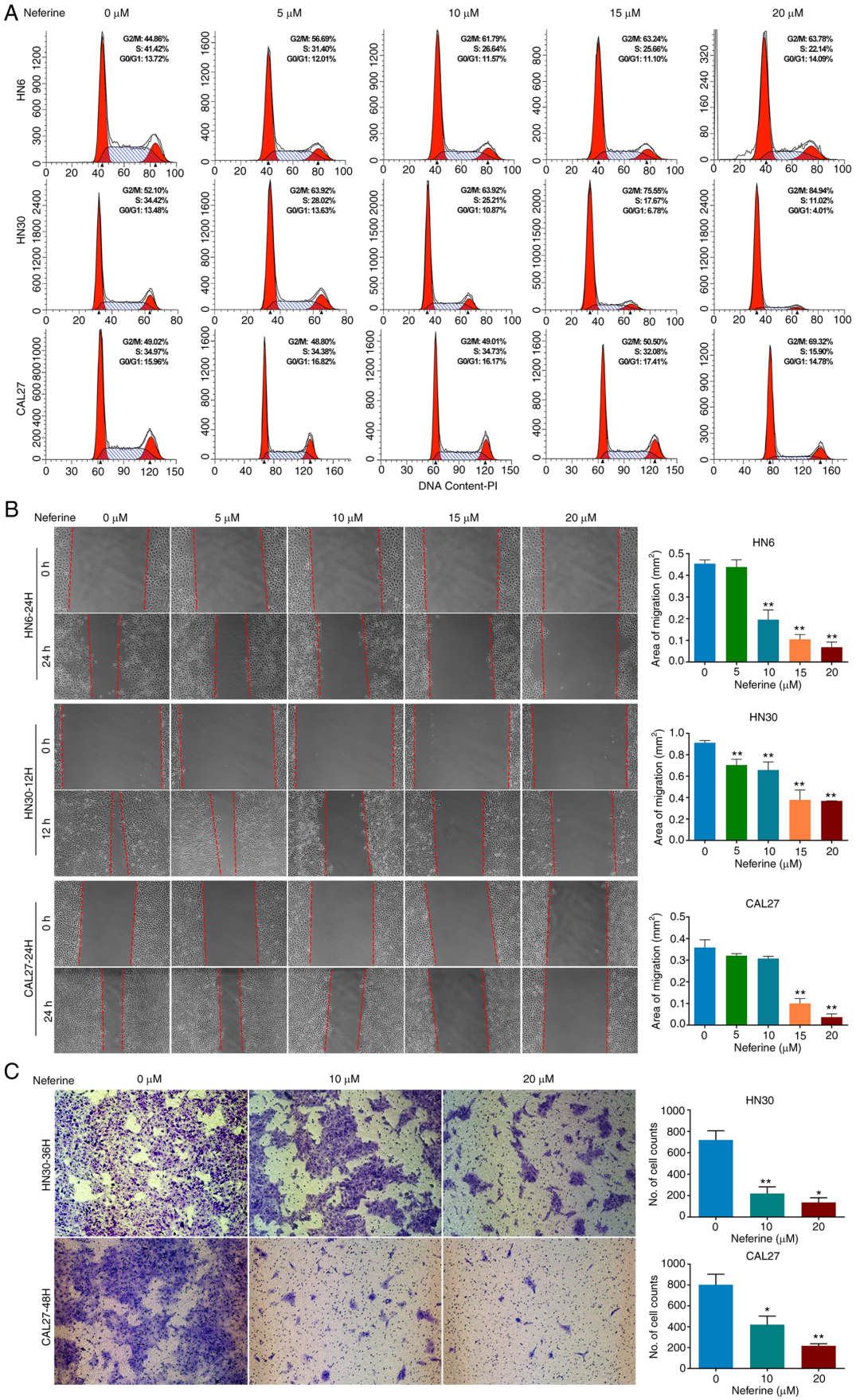

Figure S2. (A) Effect of neferine on the proportion of apoptotic HNSCC cells, as evaluated via flow cytometry. (B) Bcl-2/BAX ratio as well as caspase-8, caspase-9, caspase-3, and PARP-1 cleavage levels following treatment of HNSCC cells with various concentrations of neferine for the indicated time periods. *P<0.05. HNSCC, head and neck squamous cell carcinoma.

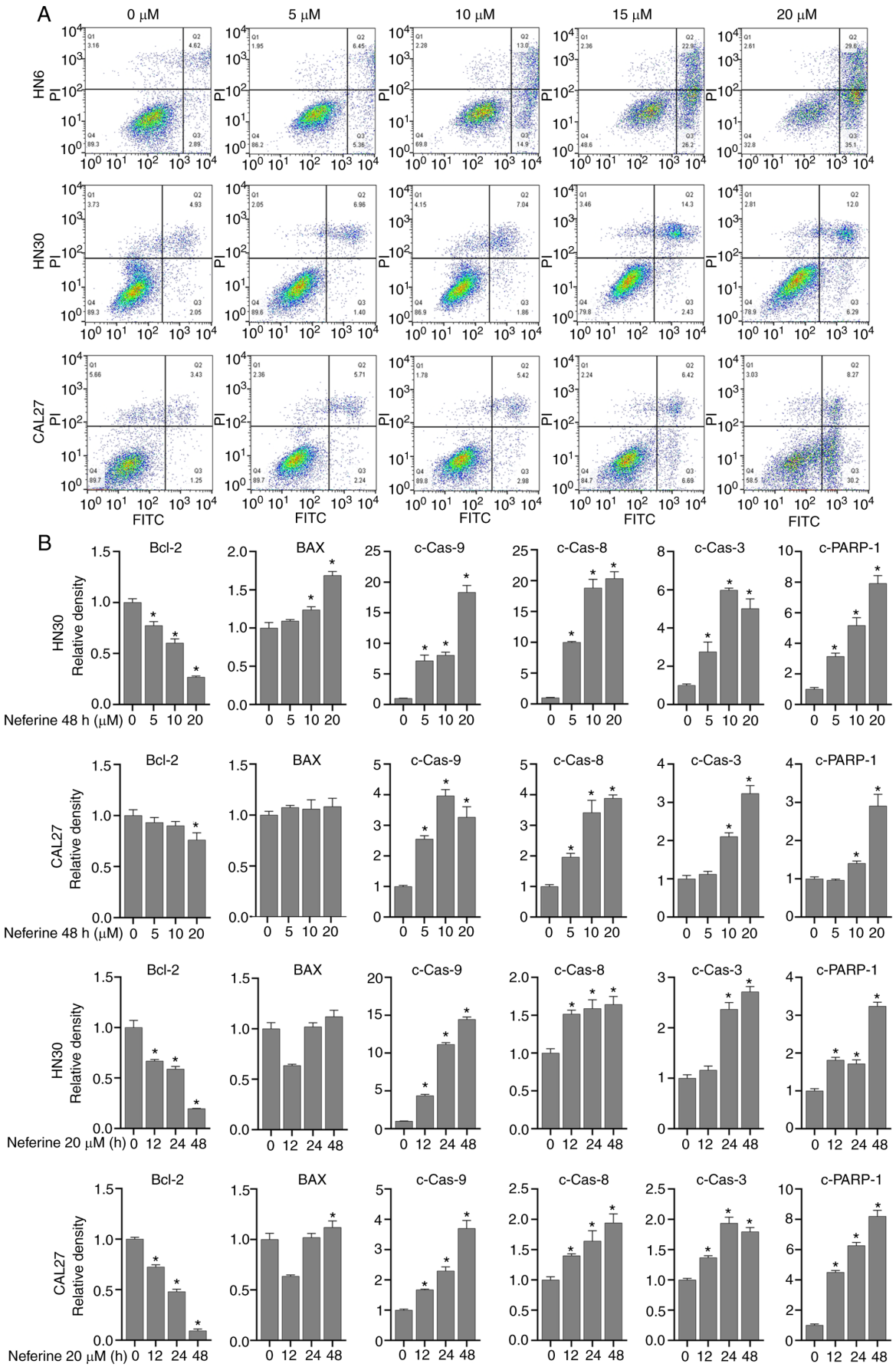

Figure S3. (A) Conversion of LC3-I to LC3-II and p62 protein expression in HN30 and CAL27 cells following neferine treatment. (B) LC3-II and p62 expression levels following co-treatment of HN30 and CAL27 cells with neferine and chloroquine. *P<0.05. CQ, chloroquine.

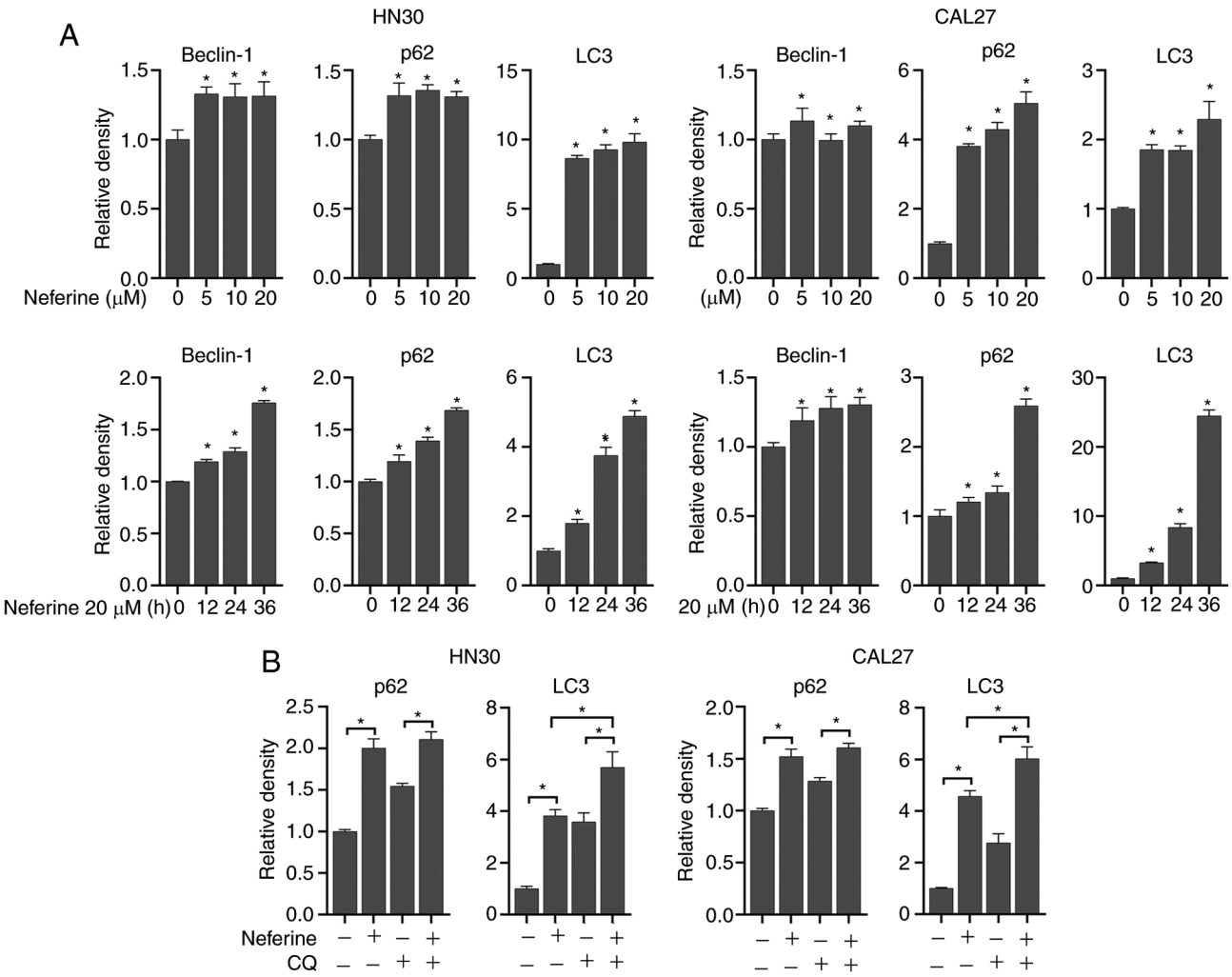

Figure S4. (A) Effect of chloroquine-mediated autophagy flux inhibition on neferine-induced apoptosis. (B) Effect of autophagic flux inhibition by chloroquine on the cleavage of caspase-8, caspase-3, and PARP1. (C) Expression of cleaved apoptosis-related proteins, caspase-8, caspase-3, PARP1, and caspase-9, following p62 knockdown. *P<0.05. si-, small interfering; CQ, chloroquine.